

## Article

# Investigating the Diurnal Variation in Coastal Boundary Layer Winds on Hainan Island Using Three Tower Observations

Ziqiang Duan <sup>1,2</sup>, Bingke Zhao <sup>1,2</sup>, Shiwang Fu <sup>3</sup>, Shuai Zhang <sup>1,2</sup>, Limin Lin <sup>1,2</sup> and Jie Tang <sup>1,2,\*</sup>

<sup>1</sup> Shanghai Typhoon Institute and Key Laboratory of Numerical Modeling for Tropical Cyclone, China Meteorological Administration, Shanghai 200030, China

<sup>2</sup> Asia-Pacific Typhoon Collaborative Research Center, Shanghai 200030, China

<sup>3</sup> Sanya Meteorological Bureau of Hainan Province, Sanya 572000, China

\* Correspondence: tangj@typhoon.org.cn

**Abstract:** This study analyzes wind structures up to 509 m in the atmospheric boundary layer in the coastal area of Hainan Island, using a dataset obtained from ultrasonic anemometers housed in three towers. The wind profile, consisting of the measurements from the three towers, followed logarithmic law. In a diurnal variation, the maximum wind speed occurred at night, with a greater component of northerly wind, while the minimum wind speed was observed at noon, with a greater component of easterly wind. The variation in wind speed suggests that the measurements were representative of the wind field in the upper part of the atmospheric boundary layer, and the variation in wind direction might be affected by sea and land breezes, which can be induced by the different thermal conditions of underlying surfaces. The diurnal variation in average wind speed ranged from 0.5 to 1.5 m s<sup>-1</sup>, and the diurnal variation in wind direction was 10–20 degrees. In our measurements, the diurnal trajectory of the wind vector was observed to be counterclockwise, which differs from previous studies conducted over uniform and flat underlying surfaces. This is partially due to the different thermodynamic conditions of the underlying land and sea surfaces. The impact of topographic relief on wind measurement is also discussed. The measurements suggest that wind speeds at altitudes above 50 m are less influenced by terrain. The height of the reversal layer, which is generated by the different diurnal variations in wind speed in the upper and lower parts of the boundary layer, was estimated to be around 300 m.

**Keywords:** wind structure; boundary layer; diurnal variation; high tower



**Citation:** Duan, Z.; Zhao, B.; Fu, S.; Zhang, S.; Lin, L.; Tang, J.

Investigating the Diurnal Variation in Coastal Boundary Layer Winds on Hainan Island Using Three Tower Observations. *Atmosphere* **2023**, *14*, 751. <https://doi.org/10.3390/atmos14040751>

Academic Editor: Nicole Mölders

Received: 13 March 2023

Revised: 8 April 2023

Accepted: 19 April 2023

Published: 21 April 2023



**Copyright:** © 2023 by the authors. Licensee MDPI, Basel, Switzerland. This article is an open access article distributed under the terms and conditions of the Creative Commons Attribution (CC BY) license (<https://creativecommons.org/licenses/by/4.0/>).

## 1. Introduction

The exchange of momentum and energy between the air and the surface, wind disasters, and the use of wind energy are all closely linked to wind structure in the atmospheric boundary layer (ABL). Therefore, it is essential to investigate the features of the wind profile, and the diurnal variation in wind speed and direction in the ABL to improve parameterization in numerical models, maximize the use of wind energy, and reduce the effects of wind disasters. In recent decades, researchers have employed various methods, such as observation, theoretical analysis, and model simulation, to understand the characteristics of wind structure in the ABL [1–7].

On a uniform and flat surface, wind is typically stronger in the lower layer during the daytime and weaker in the upper layer. This pattern reverses at night. Many field observations and simulations have supported these claims, attributing the reason to the daily changes in turbulence within the ABL. The diurnal variation in wind speeds typically ranges between 1 and 3 m s<sup>-1</sup>, with the highest variability located in the middle layer [8,9]. Additionally, the diurnal pattern of wind direction exhibits a clockwise ellipse [1,10,11].

However, with a heterogeneous underlying surface, the differences among their thermodynamic conditions must be taken into account, in addition to turbulence. The

most widely studied issue is sea and land breezes [12–15], which are generated due to the different thermodynamic conditions of the underlying surface and have been extensively studied for their strength, duration, frequency of occurrence, and effects on pollutant transport [16–21].

Recent experiments have been carried out on special underlying surfaces such as prairies, plateaus, valleys, and oceans [22–25], but few experiments have been conducted in areas such as the Hainan coast, which has multiple types of underlying surfaces and is affected by sea and land breezes, valley winds, and monsoons. It is necessary to investigate the similar or different features of the wind field over such complex underlying surfaces and to investigate the factors contributing to such differences in comparison to uniform and flat underlying surfaces. Furthermore, in previous experiments, most observations have been conducted using a single tower, and the comparison or validation of measurements obtained from two or more towers has been rare. Therefore, in this study, we aim to investigate the diurnal variation of the wind field in the coastal area of Hainan Island using data from three towers from October to November 2020.

We provide a brief description of the experiment in Section 2, and analyze the wind structure characteristics in Section 3. The results are discussed in Section 4, and the summary is presented in the last section.

## 2. Experiments

Between 4 October and 22 November 2020, measurements were conducted using three 100-m towers located in Sanya, Hainan province (Figure 1). The towers are positioned on the coastal mountains in the southernmost part of Hainan Island at coordinates (109°35′13″ E, 18°13′12″ N), (109°35′30″ E, 18°13′06″ N), and (109°35′48″ E, 18°12′59″ N), with respective elevations of 421 m, 388 m, and 275 m (Table 1). The towers are approximately arranged in a line, with about 500 m between each one. Tower 3 is the closest to the sea, approximately 1300 m away from the coastline.

**Table 1.** The longitudes, latitudes, and altitudes of the three towers.

	Longitude	Latitude	Altitude
Tower 1	109°35′13″ E	18°13′12″ N	421 m
Tower 2	109°35′30″ E	18°13′06″ N	388 m
Tower 3	109°35′48″ E	18°12′59″ N	275 m

The measurement equipment employed in this study comprised sonic anemometers (Gill WindMaster Pro, Gill Instruments Limited, Hampshire, UK), an Automatic Weather Station (AWS, Gill GMX600, Gill Instruments Limited, Hampshire, UK), and a Heavy-Duty wind monitor (HD monitor, Young 05108, R. M. Young Company, Traverse City, MI, USA). Each tower was equipped with five sonic anemometers mounted using cantilever brackets at heights of 10, 30, 50, 70, and 100 m. Two HD monitors were situated at heights of 30 and 100 m, respectively, and an AWS was positioned at a height of 30 m for each tower. Signals from these instruments were acquired using a CR6 data-acquisition system (Campbell Scientific Inc., Logan, UT, USA). The sonic anemometers were operated at a frequency of 20 Hz to measure the three-dimensional wind velocity. The average wind speed and wind direction were obtained using the HD monitor and AWS with a sampling interval of 10 min.

In quality control (QC) for the data of the sonic anemometer, we eliminated samples with missing values exceeding 1%. Following the QC method, we obtained 181,642 5-min samples from the 15 anemometers, accounting for 84.1% of all the samples. Precipitation was the primary cause of invalid data. Without precipitation, 98.9% of the data were effective; in the presence of precipitation, only 48.2% of samples were effective. The time series of wind speed during the measurement is shown in Figure 2. Over the 50-day observation period, six tropical cyclones (TCs) passed through the South China Sea, affecting the wind field around the station. These TCs were severe tropical storm “Nangka” (11–14 October

2016), 18th tropical depression (16 October 2016), typhoon “Saudel” (24–26 October 2017), severe typhoon “Molave” (28–29 October 2018), super typhoon “Goni” (6 November 2019), and severe typhoon “Vamco” (14–16 November 2022), respectively. As sonic anemometers, HD monitors, and AWS were located at 30 m height for each tower, data from this level were used to compare the wind speed obtained by different instruments. The measurements from the three monitors produced similar results, as shown in Figure 2. The correlation between wind speed from the sonic anemometer and HD monitor was 99.8%, while the correlations between the sonic anemometer and AWS were greater than 99.5% for all three towers. The correlations of wind direction between the sonic anemometer and HD monitor were 90.6% (Tower 1), 95.7% (Tower 2), and 99.6% (Tower 3), and those between the sonic anemometer and AWS were 87.8% (Tower 1), 93.3% (Tower 2), and 99.9% (Tower 3). The differences in average wind speed between the sonic anemometer and HD monitor were  $0.35 \text{ m s}^{-1}$ ,  $0.24 \text{ m s}^{-1}$ , and  $0.36 \text{ m s}^{-1}$  for the three towers, and  $0.007 \text{ m s}^{-1}$ ,  $0.029 \text{ m s}^{-1}$ , and  $0.096 \text{ m s}^{-1}$  between the sonic anemometer and AWS. These results suggest that observations from the sonic anemometer are comparable to those from the HD monitor and AWS, and can be used to describe the wind field in the area around the towers.

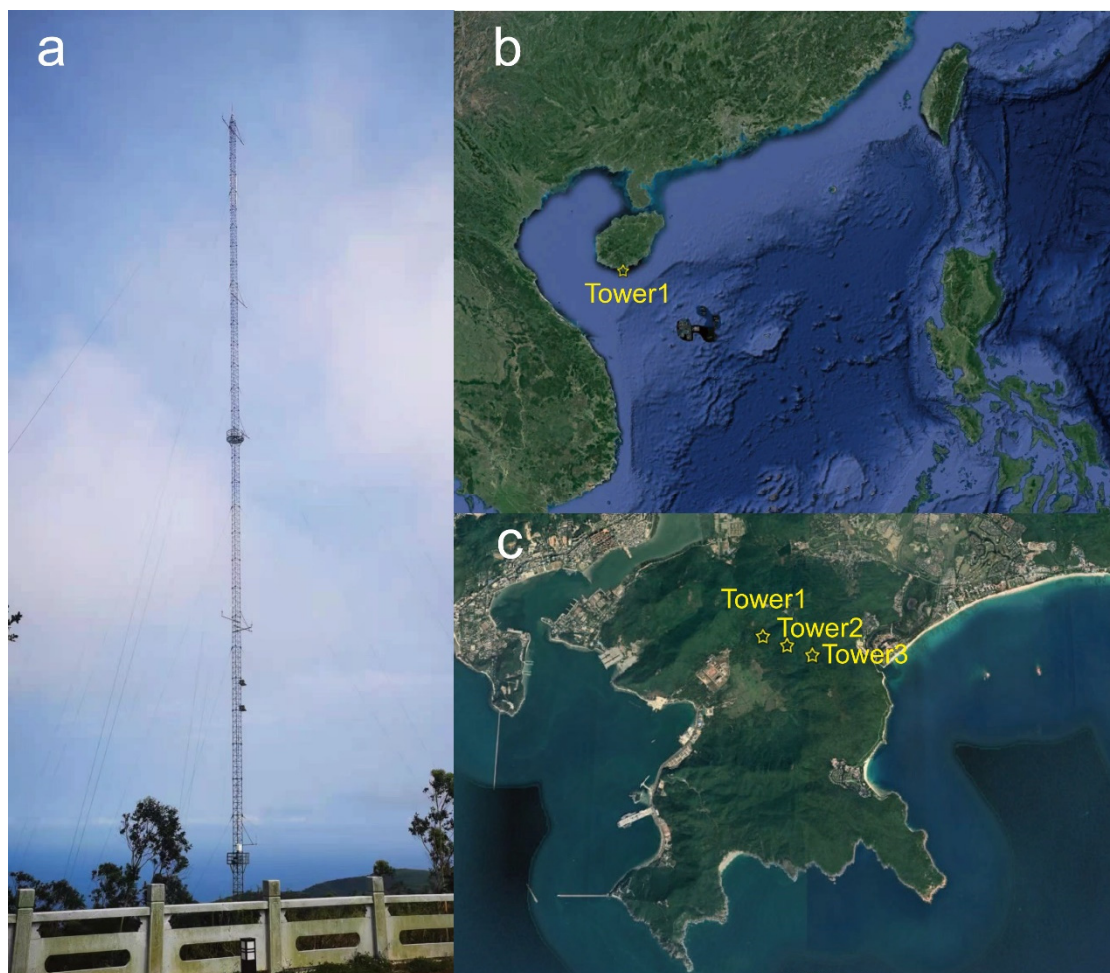


**Figure 1.** (a) Tower 1; (b) The location of measurement sites; (c) The location of the towers.

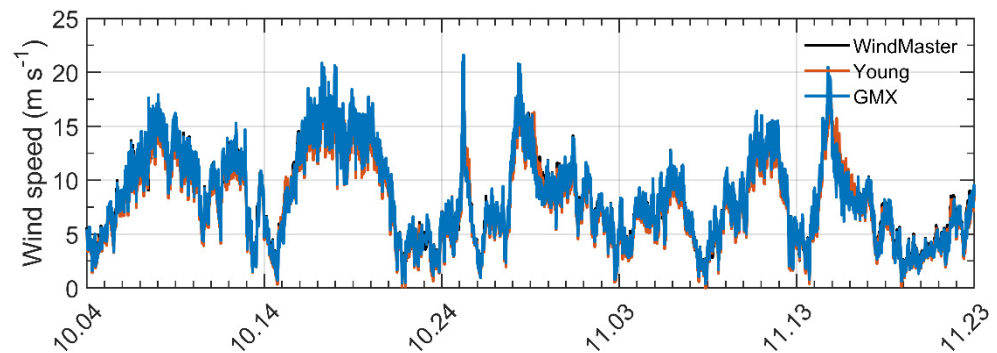


**Figure 2.** The wind speed at 30 m height. Black line: measured by sonic anemometers; Orange line: measured by HD monitor; Blue line: measured by AWS.

During the observation period, the winter monsoon in the South China Sea was gradually established, resulting in a dominant northeasterly wind direction. However, the six tropical cyclone activities in the SCS had a significant impact on the wind field around the station, with the wind structure of tropical cyclones differing substantially from general conditions. The diurnal variation of the wind field, relative distance from the TC center, relative azimuthal position, and TC intensity all contributed to changes in wind profiles. To distinguish the impact of TCs, we classified data into two groups and removed samples affected by TCs. Samples obtained within 500 km of the TC center were classified as being affected by TCs, while the rest were classified as not being affected. Only wind profiles without missing data were selected for analysis, and the number of samples for each tower is shown in Table 2. Data in the bottom layer of each tower were not considered, as they were greatly interfered with by surface vegetation.

**Table 2.** Summary of the number of samples.

	All Samples	5–10 m s <sup>−1</sup>	>10 m s <sup>−1</sup>
Tower 1	9760	4081	3466
Tower 2	8942	4099	2396
Tower 3	10,414	4356	2491

### 3. Results

#### 3.1. Wind Profile

The wind structure was analyzed using data obtained from a sonic anemometer. The dataset was divided into samples of 5-min length, with samples having wind speeds greater than 10 m s<sup>−1</sup> classified as the high-speed group, and those with wind speeds between 5 and 10 m s<sup>−1</sup> classified as the low-speed group. The vertical profiles of wind speeds in the boundary layer were plotted in Figure 3. The mean wind speed observed at the third, fourth, and fifth logarithmic layers increased with height under logarithmic wind law [8,9]. However, the wind speed at the second layer (30 m height) was significantly lower due to the impact of surface vegetation, and deviated from logarithmic wind law. The wind profile of the nine layers, which combined the upper three layers of three towers, also followed logarithmic wind law, indicating that measurements at the upper three layers of each tower were less affected by the land surface, and exhibited the features of the wind field at its altitude.

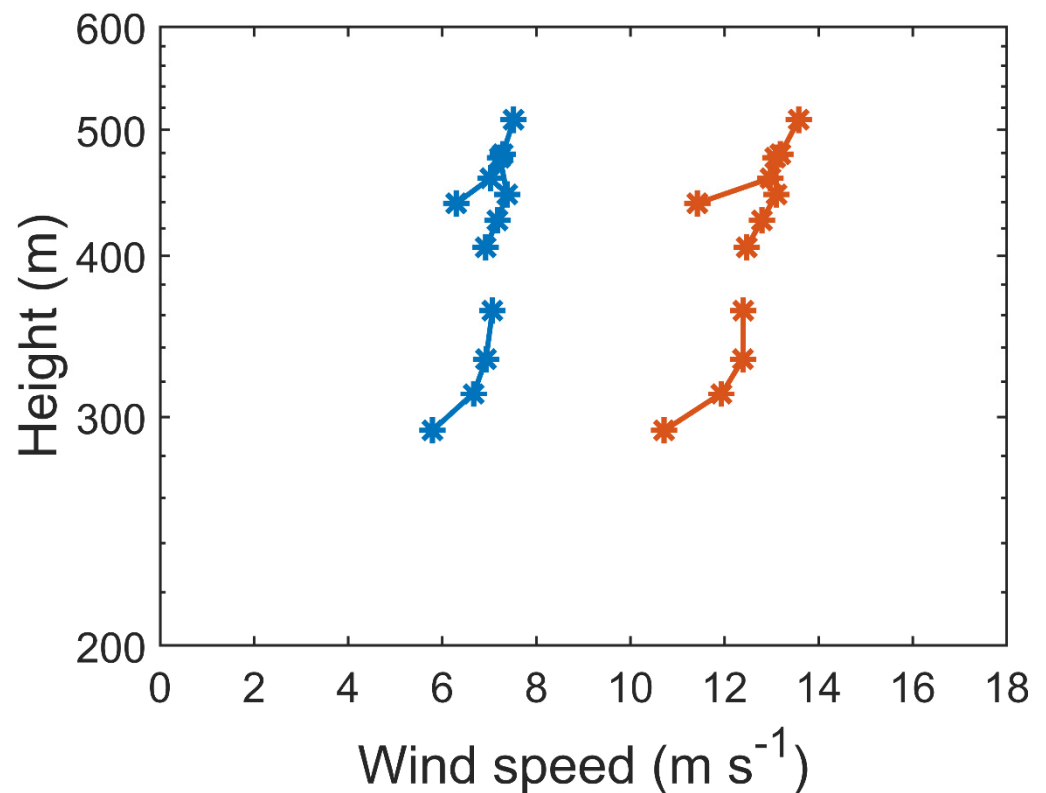


**Figure 3.** Vertical profiles of the mean wind speed ( $\text{m s}^{-1}$ ). Blue: low-speed group with wind speed between 5 and  $10 \text{ m s}^{-1}$ ; Orange: high-speed group with wind speed greater than  $10 \text{ m s}^{-1}$ .

In the high-speed group, there was a significant difference in wind speed between the three towers. Tower 1 had the highest wind speeds, while Tower 3 had the lowest. However, in the low-speed group, although Tower 2 was at a lower altitude than Tower 1, wind speeds at the second and third layers of Tower 2 were slightly higher than those of Tower 1. The trends of the wind profiles also differed between the high-speed and low-speed groups, with greater changes in wind speed with height observed in the high-speed group.

### 3.2. Diurnal Variation in Wind Fields

The diurnal variation in wind speed and wind direction at different heights was analyzed in this study. Figure 4 shows the averaged diurnal variation in wind speed and wind direction for Tower 1, Tower 2, and Tower 3. It was observed that Tower 1 and Tower 2 showed clear diurnal variations in wind speed and wind direction, while Tower 3 showed no apparent diurnal variation in wind speed. The maximum wind speed was observed at 22:00, and the minimum was around 13:00. The theory of turbulent exchange suggests that turbulence is severe during the day and weak at night, which results in effective momentum transport from the upper layer to the lower layer, making the wind at the bottom of the boundary layer stronger during the day and weaker at night [8,9]. Conversely, wind in the middle and upper layers was weaker during the day and stronger during the night. The measurements in this study were obtained at an altitude between 300 and 500 m, and the results were consistent with the theory for the middle and upper layers of the boundary layer.

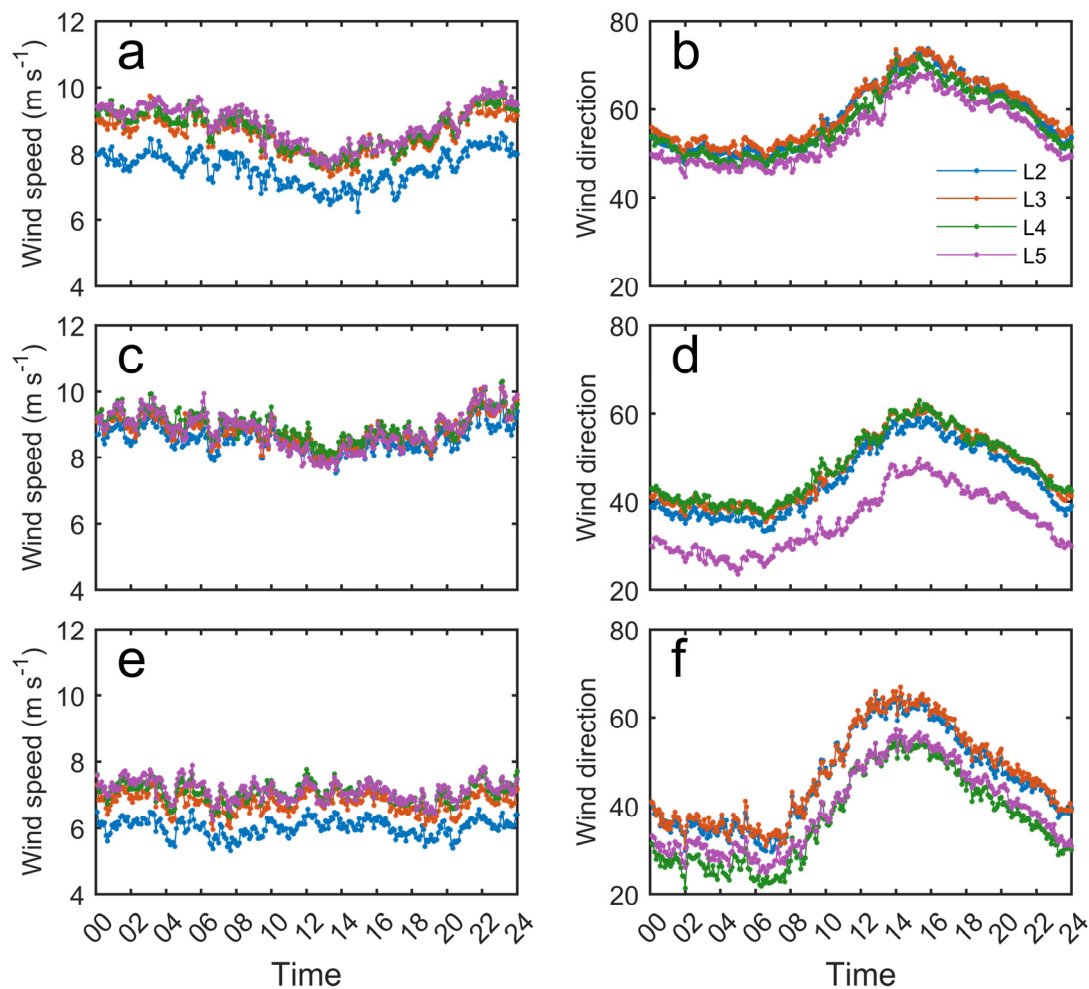


**Figure 4.** The diurnal variation in wind speed (a,c,e) and wind direction (b,d,f). (a,b): Tower 1; (c,d): Tower 2; (e,f): Tower 3. Blue line: second level; Orange line: third level; Green line: fourth level; Purple line: fifth level.

The diurnal variations in wind direction at different altitudes were similar, with a minimum at about 6 a.m. and a maximum at about 3–4 p.m. The dominant wind during the measurement period was a northeasterly wind due to the establishment of the winter monsoon from the SCS. From midnight to morning, the wind direction was lower than average, indicating a larger northerly wind component. On the other hand, the easterly wind component was greater in the afternoon. This can also be deduced from the trajectory of the wind vector (Figure 5). The variation in wind direction might be interpreted by sea and land breezes. Due to the difference in thermal conditions between the sea and land, the wind field was affected by the sea breeze, which is easterly from the sea in the afternoon. Figure 5 further indicates that the diurnal trajectory of the wind vector was counterclockwise. This was different from the clockwise rotation obtained from model simulations and observations [1,9,10]. This indicates that discrepancies or even contrary results may exist between observations and model simulations, due to environmental conditions such as monsoon, sea, and land breezes. Under conditions with a uniform and flat underlying surface, the diurnal variation of the wind vector is the result of the daily variation in turbulence intensity. However, in this study, besides turbulence, the daily variation of the wind vector was further affected by the monsoon, the sea, and land breezes, the difference in temperature between the surface layers, etc., which might be the reasons for the counterclockwise diurnal rotation of the wind vector.

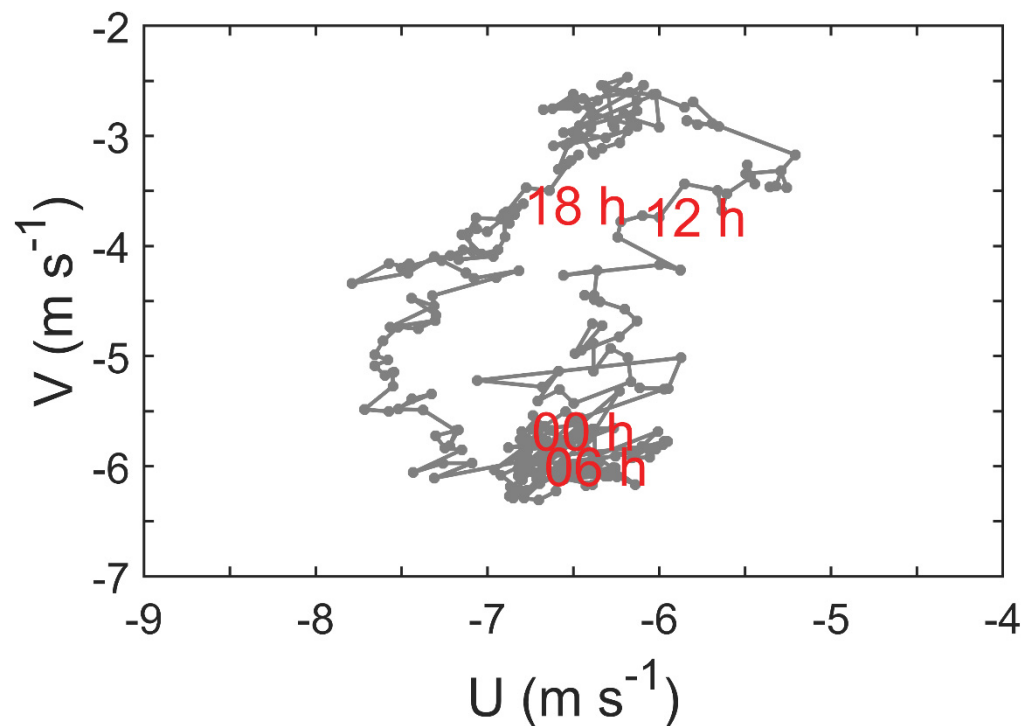


**Figure 5.** The trajectory of diurnal wind vector variation (Level 5 of Tower 1). Digit markers denote the end location of wind vectors at the corresponding time.

The diurnal variation in the wind speed at Tower 3 was not apparent compared to Tower 1 and Tower 2, but the diurnal variation in the wind direction was comparable, with similar amplitude and phase in daily variation. Previous studies have found that the phases of diurnal variation in wind speed at the bottom and upper of the boundary layer are inverse [8,9]. Wind speed at the bottom was greater at noon due to a greater turbulent exchange of momentum from the upper layer, while wind speed in the upper layer was greater at night due to less loss of momentum. Hence, an inversion layer of wind speed exists in the boundary layer. In this study, Tower 3 might have been located at the inversion height of the boundary layer, which induced the inconspicuous diurnal variation in wind speed.

### 3.3. Time of Occurrence of Maximum/Minimum

Figure 6 depicts the extreme values of wind speed and wind direction obtained by fitting their diurnal variations using trigonometric functions. The minimum wind speed was observed between 13:00 and 14:00 at Tower 1 and Tower 2, while at Tower 3, the minimum appeared after 14:00. The diurnal variation in wind direction showed a clear trend. The time of the maximum wind direction shifted towards later hours with increasing measurement height. This observation deviates from findings in studies involving uniform underlying surfaces, where the extreme value of wind direction in the upper layer was observed earlier [1]. This discrepancy may be attributed to the effects of sea and land breezes on the wind field.

It is well established that the wind field in the boundary layer of a uniform and flat underlying surface is governed by a balance between geostrophic wind and turbulent stress. The diurnal variation of the wind field is mainly caused by the variation in turbulence intensity. However, in this study, the balance between geostrophic wind and turbulent stress was affected by the presence of sea and land breezes, which might have contributed to the observed shift in the extreme values of wind direction with height.

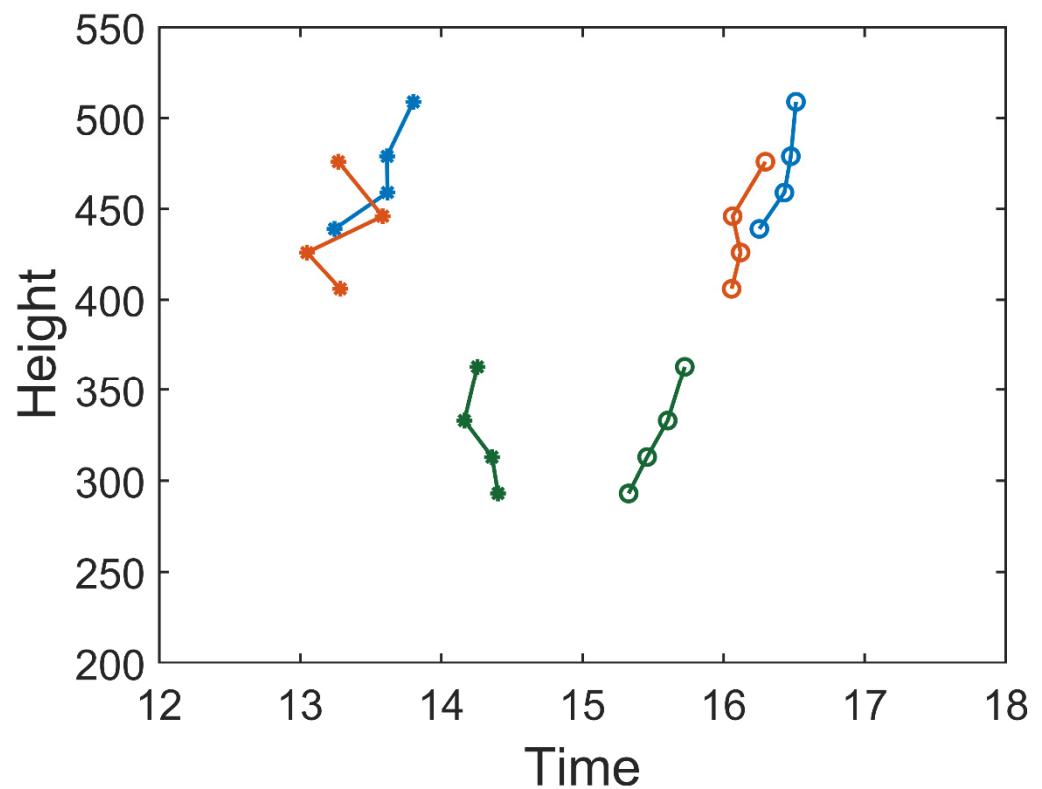


**Figure 6.** The time of extreme values of wind speed (stars) and wind direction (circles). Blue: Tower 1; Orange: Tower 2; Green: Tower 3.

### 3.4. Amplitude of Diurnal Variation

Figure 7 depicts the diurnal variation in wind speed and wind direction and the degree of variation with height. Wind speed and wind direction showed inverse trends, with the variation in wind speed increasing with height; the maximum variation in wind direction occurred at the bottom layer. Wind speed varied between 0.5 and 1.5 m s<sup>-1</sup>, which is smaller than in previous studies [8,9,11], possibly due to the average of 50 days. The variation in amplitude above 450 m was small, consistent with the theoretical model that predicts maximum amplitude in the middle layer of the boundary layer, decreasing gradually with height [8,9].

The diurnal variation in wind direction indicated the influence of sea and land breezes. The amplitude of diurnal variation was 10–20 degrees rather than 180 degrees. Wind direction variation ranges decreased with height, with Tower 3 showing noticeably greater amplitude than Towers 1 and 2. The smallest variation occurred in the fifth layer at Tower 1 (14 and −9.4 degrees) and the largest in the third layer at Tower 3 (20.1 and −16.4 degrees), consistent with previous measurements [1,3,11]. In the upper layer of the atmospheric boundary layer, the long axis of the ellipse was close to the mean wind direction (Figure 5), and wind direction variation was restricted to the angle of the short axis with a small amplitude. In the bottom layer, the angle between the mean wind and the elliptical long axis was greater, inducing a greater amplitude of wind direction.

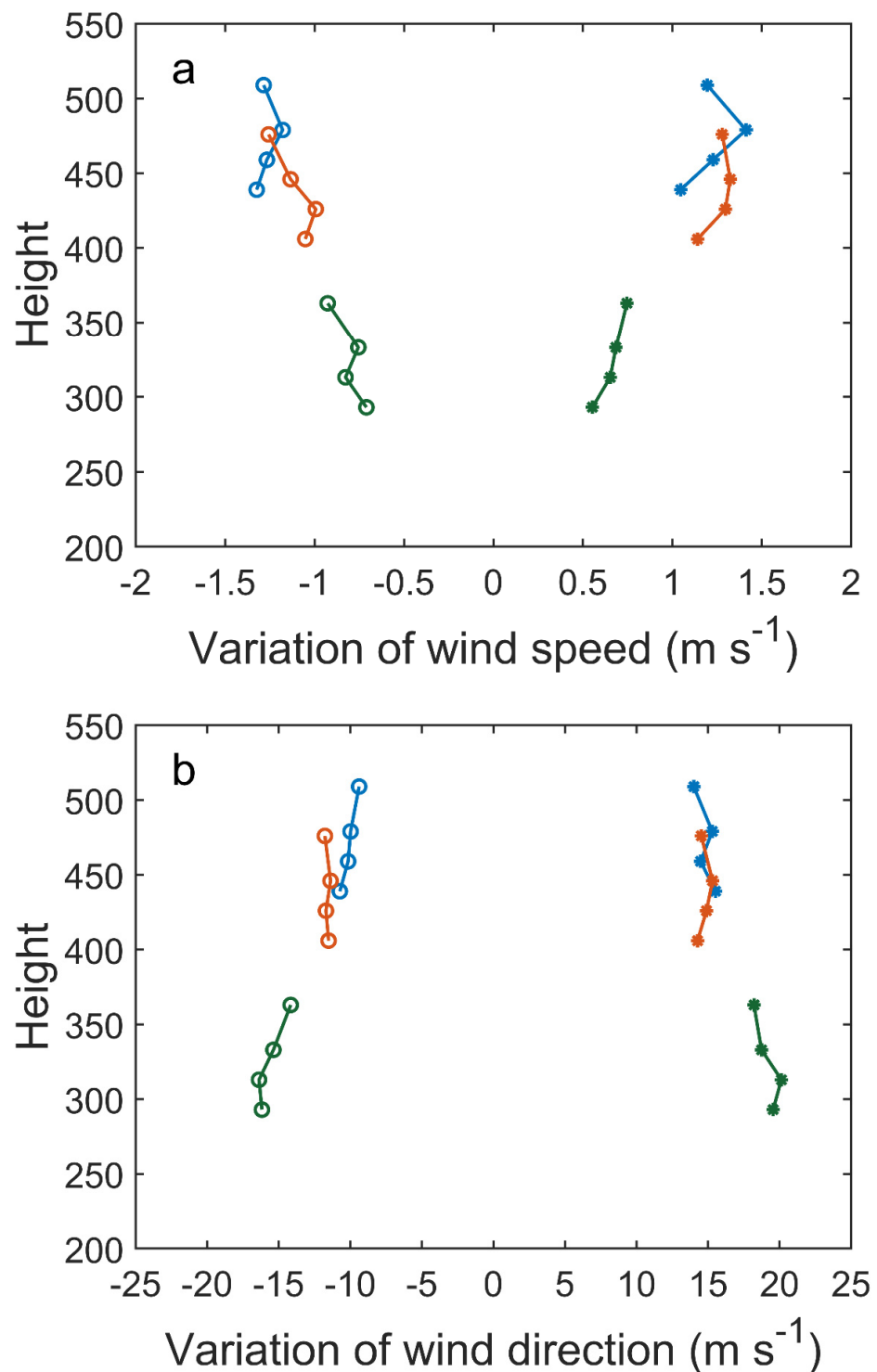


**Figure 7.** The range of diurnal variation in the mean wind speed (a) and wind direction (b). Circles: the difference between the minimum and the mean values; Stars: the difference between the maximum and the mean values. Blue: Tower 1; Orange: Tower 2; Green: Tower 3.

**4. Discussion**

The measurements were taken at three towers, each with five observation layers. The measurements taken in the three upper layers of each tower exhibited consistency with logarithmic wind law, and the wind profiles of the nine layers combined across the three towers also followed logarithmic law, which suggests that the measurements yielded reasonable results regarding the wind structure of the ABL. However, it should be noted

that the profile of the three secondary layers deviated significantly from logarithmic law. This may indicate that the wind in the second layer was sensitive to topographic relief, and at heights above 50 m, the magnitude of wind speed was less influenced.

Based on the theoretical model, wind speeds are greater during the daytime and smaller at night at the bottom of the ABL; the opposite is true for the upper part of the ABL. Our study found that wind speeds were smaller during the daytime and greater at night, which aligns with the diurnal variation in wind speed at the upper part of the ABL. This suggests that our measurements were representative of the wind field at the upper part of the ABL, which also indicates that the wind speed at the upper layers of the tower was less influenced by the topographic relief.

The theoretical model also indicates that there is a reversal layer between the upper and lower part of the ABL due to the different trends of the diurnal variation in wind speed. In this study, the diurnal variation in wind speed at Tower 3 was not obvious. This might be because Tower 3 was located in the reversal layer, indicating that the height of the reversal layer was around 300 m. However, without measurements at a height below 300 m, we did not obtain the contrary phase of the diurnal variation at different altitudes. It is necessary to conduct more observations to investigate the reversal height in the ABL.

The daily trajectory of the wind vector is a clockwise ellipse, due to the daily variation in turbulence [1,3,11] under conditions with a uniform and flat underlying surface. However, in our measurement, the trajectory of the wind vector was counterclockwise. This indicated that under conditions with a non-uniform underlying surface, factors such as different thermal conditions of the underlying surface and monsoon could induce different or even contrary trends of the diurnal variation in wind. In our analysis of the diurnal variation in wind direction, we found that the wind direction was influenced by differing thermodynamic conditions of the underlying land and sea surfaces. This factor may have also contributed to the characteristics of the trajectory of the wind vector in our measurements.

Through measurements taken at different altitudes, we quantitatively obtained the amplitude of diurnal variations in wind speed and wind direction. Our results show that the amplitude of wind speed increased with height, but the trend of wind direction was inverse. The profiles of amplitudes can be interpreted by the turbulent exchange in the ABL and were consistent with previous measurements. Even though the wind was affected by sea and land breezes, during the dominance of winter monsoon, the angle variation induced by sea and land breezes was less than 20 degrees rather than 180 degrees. This means that the effect of the background wind field cannot be neglected when studying the research related to sea and land breezes, such as the pollutant diffusion, momentum, and energy transport in the ABL.

## 5. Summary

In this study, we investigated the characteristics of a wind field with a complex underlying surface by obtaining measurements from three towers located on the coastal mountains of Hainan Island. The area around the sites contains sea and hills, which could affect the wind field via sea and land breezes, valley wind, and monsoon. We collected measurements at heights up to 509 m to quantify the diurnal variations of the wind field and analyze the vertical characteristics of these variations during the winter monsoon.

We began by comparing the results obtained from different instruments to ensure their reliability. The correlations between wind speeds obtained from different instruments were greater than 99.5%, and the correlation for wind direction measurements ranged from 87.8% to 99.9%. The average differences in wind speed measurements among different instruments were smaller than  $0.36 \text{ m s}^{-1}$ . Additionally, the wind profile taken from the measurements from the three towers followed logarithmic law. These results show that observations from the sonic anemometer, HD monitor, and AWS are comparable, and can be used to describe the wind structure in the area around the towers.

We analyzed the characteristics of the diurnal variation of the averaged wind structure and found that the maximum wind speed occurred at night with a greater component of northerly wind, while the minimum wind speed was observed at noon with a greater component of easterly wind. The variation in wind speed suggests that the measurements were representative of the wind field at the upper part of the ABL. Additionally, the variation in wind direction might be affected by the sea and land breezes, which were induced by the different thermal conditions of underlying surfaces. The time at which the wind speed reached its extreme value was earlier at a higher height, while the time for wind direction was later with increasing height. The diurnal variation in averaged wind speed ranged from 0.5 to 1.5 m s<sup>-1</sup>, and the diurnal variation in wind direction was 10–20 degrees. The amplitude of wind speed increased with height; the amplitude of wind direction decreased with height. However, the amplitude values were smaller compared to previous studies, possibly due to the averaging of data over 50 days.

The impact of topographic relief on wind measurement was also discussed. The measurements suggest that wind speeds above 50 m were less influenced by terrain. This was induced by the fact that the wind profile consisted of the three secondary layers that deviated from logarithmic law, while the profile consisted of nine upper layers that followed logarithmic law. Furthermore, we observed that wind speed was greater at night, depicting the characteristics of the wind structure of the upper boundary layer, and suggesting that the measurements were less affected by topographic relief.

Our measurements revealed some differences in wind structure compared to previous studies conducted over uniform and flat underlying surfaces. We observed a counterclockwise diurnal trajectory of the wind vector, which differs from previous findings. This might be partially attributed to the different thermodynamic conditions of the underlying land and sea surfaces.

The diurnal variations in wind speed in the upper and lower parts of the boundary layer differ, resulting in a reverse layer in the middle level of the ABL. The identification of the height of the reversal layer is meaningful to the understanding of turbulent exchange and the further development of the parameterization scheme in the ABL. However, determining this height can be quite challenging, due to observational difficulties. In this study, we estimated the height of the reversal layer to be around 300 m.

Although our study provides insights into the diurnal variation in wind structure in the ABL, some limitations should be acknowledged. In our measurements, as the data were obtained at an altitude between 300 m and 500 m, the full vertical features of the wind field were not analyzed without the measurements at the bottom layer of the ABL. Furthermore, the observations were conducted during the latter half of the year, reflecting the characteristics of the wind field under the domination of the winter monsoon. To gain a more complete understanding of the wind structure in the ABL, further experiments and analysis are needed, particularly during periods with summer monsoon or tropical cyclones.

**Author Contributions:** Conceptualization, J.T.; Methodology, Z.D. and J.T.; Software, Z.D.; Validation, Z.D.; Formal analysis, Z.D.; Investigation, Z.D., B.Z., S.F., S.Z., L.L. and J.T.; Resources, J.T.; Data curation, B.Z., S.F., S.Z., L.L. and J.T.; Writing—original draft, Z.D.; Writing—review & editing, J.T.; Visualization, Z.D.; Supervision, J.T.; Project administration, B.Z. and J.T. All authors have read and agreed to the published version of the manuscript.

**Funding:** This research was funded by the National Key R&D Program of China under grants (2021YFC3000803, 2018YFB1501104), the National Natural Science Foundation of China under grants (41806046, 41775064), Program of Shanghai Academic/Technology Research Leader (21XD1404500), and the Scientific Research Program of Shanghai Science and Technology Commission under grant (19dz1200101). This research was also supported by the ESCAP/WMO Project (EXOTICCA).

**Institutional Review Board Statement:** Not applicable.

**Informed Consent Statement:** Not applicable.

**Data Availability Statement:** Not applicable.

**Acknowledgments:** The authors are grateful to two anonymous reviewers for their constructive review comments, which helped improve the manuscript.

**Conflicts of Interest:** The authors declare no conflict of interest.

## References

1. Holton, J.R. The diurnal boundary layer wind oscillation above sloping terrain. *Tellus* **1967**, *19*, 200–205. [[CrossRef](#)]
2. Deardorff, J.W. Numerical Investigation of Neutral and Unstable Planetary Boundary Layers. *J. Atmos. Sci.* **1972**, *29*, 91–115. [[CrossRef](#)]
3. Sheih, C.M. A Theoretical Study of the Diurnal Wind Variations in the Planetary Boundary Layer. *J. Atmos. Sci.* **1972**, *29*, 995–998. [[CrossRef](#)]
4. Liu, S.; Liang, X. Observed Diurnal Cycle Climatology of Planetary Boundary Layer Height. *J. Clim.* **2010**, *23*, 5790–5809. [[CrossRef](#)]
5. Baklanov, A.A.; Grisogono, B.; Bornstein, R.; Mahrt, L.; Zilitinkevich, S.S.; Taylor, P.; Larsen, S.E.; Rotach, M.W.; Fernando, H.J.S. The Nature, Theory, and Modeling of Atmospheric Planetary Boundary Layers. *Bull. Am. Meteorol. Soc.* **2011**, *92*, 123–128. [[CrossRef](#)]
6. Svensson, G.; Holtslag, A.A.M.; Kumar, V.; Mauritsen, T.; Steeneveld, G.J.; Angevine, W.M.; Bazile, E.; Beljaars, A.; de Bruijn, E.I.F.; Cheng, A.; et al. Evaluation of the Diurnal Cycle in the Atmospheric Boundary Layer Over Land as Represented by a Variety of Single-Column Models: The Second GABLS Experiment. *Bound. Layer Meteorol.* **2011**, *140*, 177–206. [[CrossRef](#)]
7. Holtslag, A.A.M.; Svensson, G.; Baas, P.; Basu, S.; Beare, B.; Beljaars, A.C.M.; Bosveld, F.C.; Cuxart, J.; Lindvall, J.; Steeneveld, G.J.; et al. Stable Atmospheric Boundary Layer and Diurnal Cycles: Challenges for Weather and Climate Models. *Bull. Am. Meteorol. Soc.* **2013**, *94*, 1691–1706. [[CrossRef](#)]
8. Stull, R.B. *An Introduction to Boundary Layer Meteorology*; Springer: Dordrecht, The Netherlands, 1988.
9. Garratt, J.R. *The Atmospheric Boundary Layer*; Cambridge University Press: New York, NY, USA, 1992.
10. Malcher, J.; Kraus, H. Low-level jet phenomena described by an integrated dynamical PBL model. *Bound. Layer Meteorol.* **1983**, *27*, 327–343. [[CrossRef](#)]
11. Baas, P.; Bosveld, F.C.; Baltink, H.K.; Holtslag, A.A.M. A Climatology of Nocturnal Low-Level Jets at Cabauw. *J. App. Meteorol. Clim.* **2009**, *48*, 1627–1642. [[CrossRef](#)]
12. Simpson, J.E. *Sea Breeze and Local Winds*; Cambridge University Press: Cambridge, UK, 1994.
13. Miller, S.T.K.; Keim, B.D.; Talbot, R.W.; Mao, H. Sea breeze: Structure, forecasting, and impacts. *Rev. Geophys.* **2003**, *41*, 1011. [[CrossRef](#)]
14. Crosman, E.T.; Horel, J.D. Sea and Lake Breezes: A Review of Numerical Studies. *Bound. Layer Meteorol.* **2010**, *137*, 1–29. [[CrossRef](#)]
15. Crosman, E.T.; Horel, J.D. Idealized Large-Eddy Simulations of Sea and Lake Breezes: Sensitivity to Lake Diameter, Heat Flux and Stability. *Bound. Layer Meteorol.* **2012**, *144*, 309–328. [[CrossRef](#)]
16. Atkinson, B.W. *Meso-Scale Atmospheric Circulations*; Academic Press: Cambridge, MA, USA, 1981.
17. Pielke, R.A.; Segal, M. Mesoscale Circulations Forced by Differential Terrain Heating. In *Mesoscale Meteorology and Forecasting*; American Meteorological Society: Boston, MA, USA, 1986; pp. 516–548.
18. Abbs, D.J.; Physick, W.L. Sea-breeze observations and modelling: A review. *Aust. Meteorol. Mag.* **1992**, *41*, 7–19.
19. Segal, M.; Leuthold, M.; Arritt, R.W.; Anderson, C.; Shen, J. Small Lake Daytime Breezes: Some Observational and Conceptual Evaluations. *Bull. Am. Meteorol. Soc.* **1997**, *78*, 1135–1147. [[CrossRef](#)]
20. Hinrichsen, D. *Coastal Waters of the World: Trends, Threats, and Strategies*; Island Press: Washington, DC, USA, 1998; p. 298.
21. Levy, I.; Dayan, U.; Mahrer, Y. Studying Coastal Recirculation with A Simplified Analytical Land-Sea Breeze Model. *J. Geophys. Res.* **2008**, *113*, D3104. [[CrossRef](#)]
22. Yanai, M.; Li, C. Mechanism of Heating and the Boundary Layer over the Tibetan Plateau. *Mon. Weather Rev.* **1994**, *122*, 305–323. [[CrossRef](#)]
23. Liu, X.; Bai, A.; Liu, C. Diurnal variations of summertime precipitation over the Tibetan Plateau in relation to orographically-induced regional circulations Focus on Climate Change on the Tibetan Plateau. *Environ. Res. Lett.* **2009**, *4*, 45203. [[CrossRef](#)]
24. Parish, T.R.; Oolman, L.D. On the Role of Sloping Terrain in the Forcing of the Great Plains Low-Level Jet. *J. Atmos. Sci.* **2010**, *67*, 2690–2699. [[CrossRef](#)]
25. Zardi, D.; Whiteman, C.D. Diurnal mountain wind systems. In *Mountain Weather Research and Forecasting*; Springer: Berlin/Heidelberg, Germany, 2013; pp. 35–119.

**Disclaimer/Publisher’s Note:** The statements, opinions and data contained in all publications are solely those of the individual author(s) and contributor(s) and not of MDPI and/or the editor(s). MDPI and/or the editor(s) disclaim responsibility for any injury to people or property resulting from any ideas, methods, instructions or products referred to in the content.